



The Effect of Temperature Gradients on Elastic Wave Propagation in Split Hopkinson Pressure Bars

Stephen M. Walley¹

Received: 30 July 2019 / Accepted: 27 March 2020 / Published online: 15 April 2020
© The Author(s) 2020

Abstract

If it is desired to obtain high rate mechanical data of materials at non-ambient temperatures using the split Hopkinson (Kolsky) bar technique, it is necessary either to consider what effect a temperature gradient has on the propagation of elastic waves along a metallic rod or to design a mechanism that minimises the exposure of the Hopkinson bars to heating or cooling. Two main mechanical systems have been devised: the first where the bars are brought into contact with the specimen a short time (less than one second) before the specimen is dynamically loaded; the second where the specimen is moved into position just before it is dynamically loaded. As these mechanisms are complex to design and build, many researchers choose the simpler option of heating (or cooling) the ends of the bars as well as the specimen. This review summarises issues that should be considered if this option is taken.

Keywords Hopkinson bar · Temperature gradient · Elastic wave

Introduction

Some materials such as water ice only exist at cryogenic temperatures. Some may be subjected to impact when in use at high temperatures, such as the alloys used in turbines [1, 2]. Yet others may be subjected to a heat pulse at the same time as a shock in, for example, blast loading of concrete [3] or rock [4]. If such events are going to be accurately modelled, a full constitutive relation for the material of interest is needed and this in turn requires mechanical data to be obtained for that material over a wide range of temperature and strain rate [5–10]. Thus it is necessary to be able to perform high rate split Hopkinson bar (SHPB) tests at both high and low temperatures. Heating and cooling techniques for achieving this have been reviewed by Chen & Song [11]. So the emphasis of this article will not be on the experimental methods for accomplishing this but on the effect of temperature gradients on elastic wave propagation in the bars themselves. For a comprehensive overview of the SHPB technique and its applications, the reader is referred to the book by Chen & Song [12].

If the specimen (and hence the Hopkinson bar ends) are at a different temperature to ambient, there are several problems that have to be addressed.

First

The elastic modulus, E , of the Hopkinson bar rods (and hence their mechanical impedance) changes with temperature (Fig. 1). As can be seen from this figure, temperature has a significant effect even for a metallic alloy such as Inconel 718 whose elastic properties are a weak function of temperature (the decrease in modulus of about 40 GPa for a temperature rise of 600 K corresponds to a change in impedance of about 10%). The problem is much worse for Hopkinson bars made from viscoelastic polymeric materials [13–15] as their mechanical properties depend on both frequency and temperature [16–19]. Polymers have an additional problem for high temperature testing as even the most heat-resistant ones cannot be used above a few hundred degrees Celsius due to them melting and decomposing. They can, however, be used in low temperature Hopkinson bar tests [15], unless they become brittle. As far as I know, no-one has so far used polymer bars at elevated temperatures. Instead low impedance elastic metals (such as titanium or magnesium alloys [20, 21]) are usually used for obtaining high rate mechanical data

✉ Stephen M. Walley
smw14ster@gmail.com

¹ PCS Fracture and Shock Physics Group, Cavendish Laboratory, J.J. Thomson Avenue, Cambridge CB3 0HE, UK

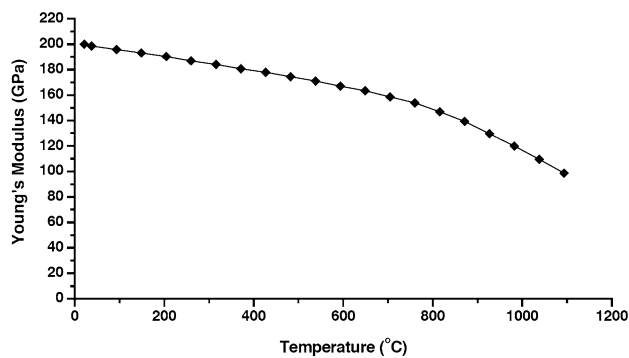


Fig. 1 Young's modulus as a function of temperature for Inconel 718 calculated from data supplied by the manufacturer. From [22]

for low strength materials. The titanium alloy Ti6Al4V also has the additional advantage that it has a relatively low thermal conductivity ($7.2 \text{ Wm}^{-1}\text{K}^{-1}$ as compared to $11.4 \text{ Wm}^{-1}\text{K}^{-1}$ for Inconel 718 and $16.5 \text{ Wm}^{-1}\text{K}^{-1}$ for stainless steel).

The change in elastic modulus has three effects:

- (i) the particle velocity, $V = F/(AZ)$, at the end of a bar of cross-sectional area, A , for a given force, F , will change (Fig. 2; [23–25]);
- (ii) some of the input pulse will be reflected from the section of the bar that is at a non-ambient temperature (Fig. 3; [25, 26]) due to the difference in impedance (the reflection coefficient, R , at an interface between two materials of different acoustic impedance is given by $R = \frac{Z_1 - Z_2}{Z_1 + Z_2}$ ([27] p. 34), where Z_1 and Z_2 are the acoustic impedances of the bar at ambient and non-ambient temperatures respectively;

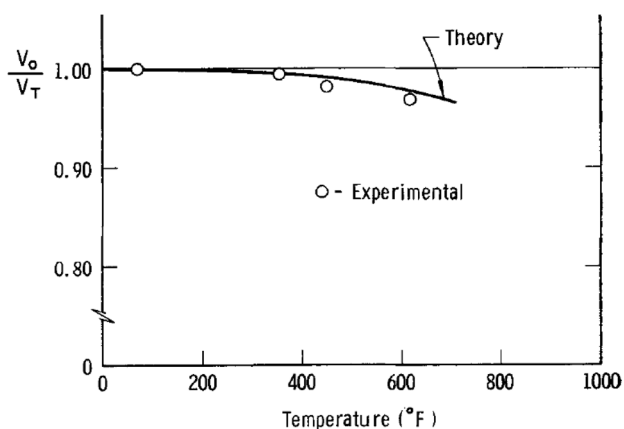


Fig. 2 Plot of the ratio of particle velocity, V_0 , at the strain gauge to the particle velocity, V_T , at the end of a high strength steel bar as a function of temperature of the heated end. From [23]

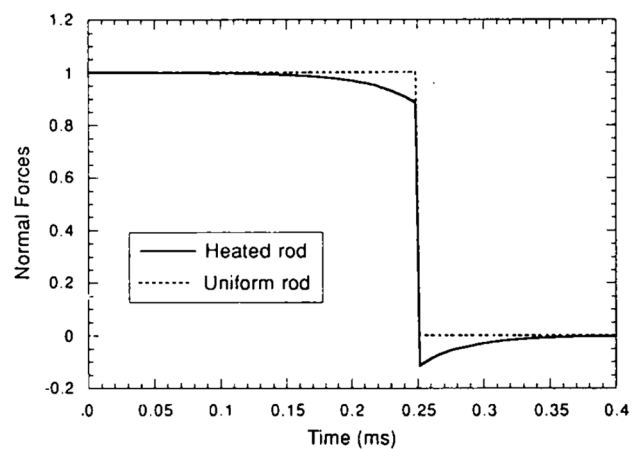


Fig. 3 Computed effect of reflection from a temperature gradient on the force measured at a strain gauge station 'upstream' of the gradient (input pulse was a Heaviside function). Solid line: heated rod. Dotted line: unheated rod. The rod was made from a refractory austenitic steel whose end was heated to $1000 \text{ }^\circ\text{C}$ [24]. From [25]

- (iii) elastic waves propagating through the temperature gradient will be distorted differently by dispersion compared to a rod that is all at the same temperature [26, 28–34].

Second

The strain gauges must be kept at ambient temperature, particularly if they are semiconductor gauges, or their response will be changed [11, 35, 36]. As most designers of Hopkinson bar systems position the strain gauges sufficiently far away from the specimen that they remain at ambient temperature, this issue is not normally a problem. However, if it is necessary to measure strains in the heated (or cooled) sections of the bars, a non-contact temperature insensitive optical technique could be used such as photon Doppler velocimetry [37–39], although this may be hard to implement close to the device used to heat or cool the specimen.

Third

If tests are to be carried out above ambient temperature, the heating rates should be as rapid as possible to avoid annealing the specimen and hence changing its internal structure [11, 40–42]. However, if the specimen is initially in a fully annealed state the heating rate will not matter. Cooling rates for cryogenic studies are not normally so critical since lowering the temperature has the effect of freezing the structure. Most researchers have, however, used conventional resistance furnaces rather than rapidly-acting induction or radiant heaters for high temperature studies e.g. [11, 23, 43–47].

Figure 3 shows the error that results in the calculation of the force on a specimen at $1000 \text{ }^\circ\text{C}$ if it is assumed that

the temperature gradient has no effect. This systematic error rises from 1.5% for $T_F=125\text{ }^\circ\text{C}$ to 12% for $T_F=1000\text{ }^\circ\text{C}$ (T_F is the temperature of the furnace). The calculation was performed using a simple form for the temperature distribution ($T(x) = T_F e^{-\mu x}$) and dividing the rod into 80 equal segments [25].

The Solutions

There have been several approaches to these problems listed above.

The first is either to ignore it [48, 49] or to say that thermal gradients in the bars have only a small effect on the measured stress pulses so that their effects are less than the experimental error (unless the temperature excursion is large; [50–53]). This is usually the case for metallic bars from liquid helium temperatures (4.2 K) [53] up to around +300 °C. For temperatures between 300 and 600 °C, Inconel Alloy 718 can be used. This alloy has a Young's modulus (and hence mechanical impedance) which is a relatively weak function of temperature over the temperature range –200 to +600 °C (see Fig. 1 and also [54]).

The second is to seek to heat only the specimen and not the bar. This is essential if it is desired to test above 600 °C.

Several ways of doing this have been devised:

- (i) heat the specimen (and a short section of the ends of the quickly by induction [41], infrared pulse heating [55–57], or by passing a current through the specimen to raise its temperature by resistance heating [58]. Note that none of these rapid heating techniques work for materials with low thermal or electrical conductivity, such as polymers [59]. Also rapid heating can produce non-uniform (and usually unknown) temperature distributions within both the specimen and the bars [57]. If both the specimen and the ends of the bars are brought to temperature, the issue arises as to whether the bar ends will be damaged by the test. This would be the case if the flow stress of the bar material falls below about one third of that of the specimen [60–62] or if the loading pulse is sufficiently strong to produce plastic rather than elastic deformation of the bar material at the temperature of interest;
- (ii) construct a mechanical device to bring the bars into contact with the heated specimen a fraction of a second before it is loaded (Fig. 4) [45], or, alternatively, slide the heated specimen into position between the bars a short time before loading [22, 63]. Note that Lindholm and Yeakley [23] had previously reported that this method cannot be done manually fast enough to avoid cooling the specimen substantially.

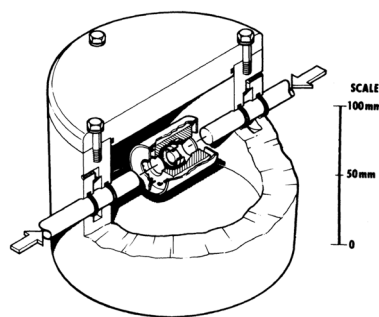


Fig. 4 Schematic diagram of a device developed at the Los Alamos National Laboratory to bring Hopkinson bar rods into contact with heated specimen. From [45]

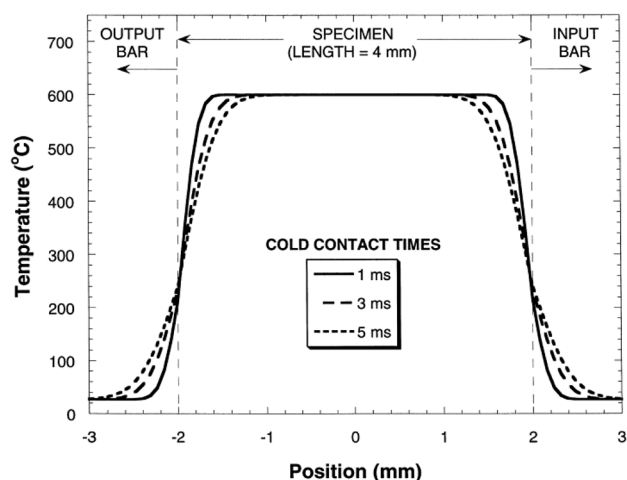


Fig. 5 Calculation of the effect of cold contact time for a specimen of vanadium heated to 600 °C. From [55]

Even a few milliseconds contact of a hot specimen with cold bars can result in a significant transfer of heat energy (Figs. 5, 6, 7, 8, 9). This technique has been used successfully up to 1000 °C [64]. High temperature tension and torsion experiments cannot be performed this way as the specimen in these cases cannot be slid in as it has to be in mechanical (and hence thermal) contact with the bars at all times [65]. For compression experiments (usually performed using light gas-guns) there can be significant uncertainty in the timings of bar contact [55] and hence in the choreography of the mechanical loading and heating pulses [11, 57].

- (iii) load the specimen through an insulator (such as alumina) which at room temperature has an impedance nearly equal to steel [66, 67] (as far as I know, this

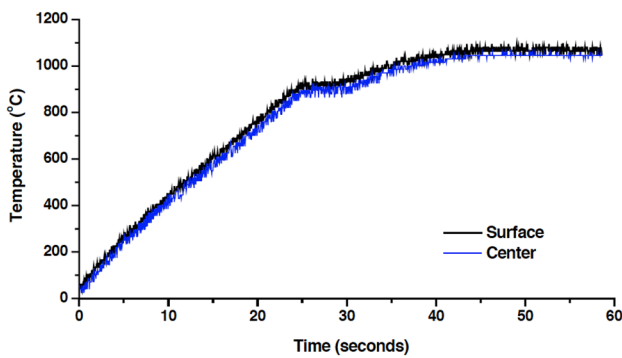


Fig. 6 Temperature–time plots for the heating of a specimen to 1000 °C using the technique shown in Fig. 7. From [22]

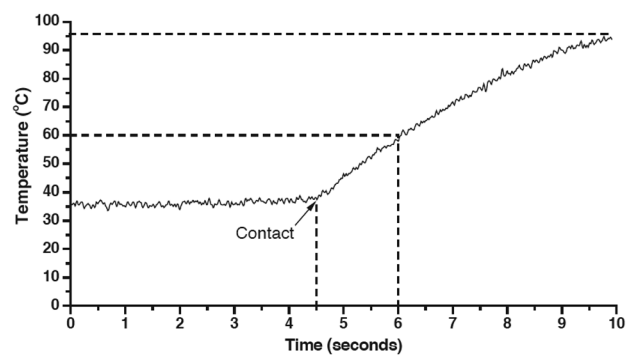


Fig. 8 Temperature–time plots of heating of the bar after bringing them into contact with a specimen heated to 1000 °C. From [22]

method so far has only been used for compression experiments);

- (iv) sandwich the specimen between two metal platens of sufficient thickness that when the bars are brought into contact with the specimen-platen sandwich, the platens rather than the specimen cool on the time-scale of the test (Figs. 10, 11) [68];
- (v) keep the impedance constant along the length of the bar by shaping it to compensate for the temperature gradient [44]. So far this has only been implemented for torsion testing and dynamic fracture testing of ceramics in an SHPB [69]. This method has the disadvantage that a bar of a particular profile can only be used for one particular (and known) temperature gradient;
- (vi) calculate the effect of the temperature gradient on the wave propagation [14, 23, 43]. One way of doing this is to determine the impedance as a function of position (see Fig. 12) [24, 25, 69] using the two-point measurement technique pioneered by Lundberg and colleagues for waves propagating down rods of changing cross-section [70, 71].

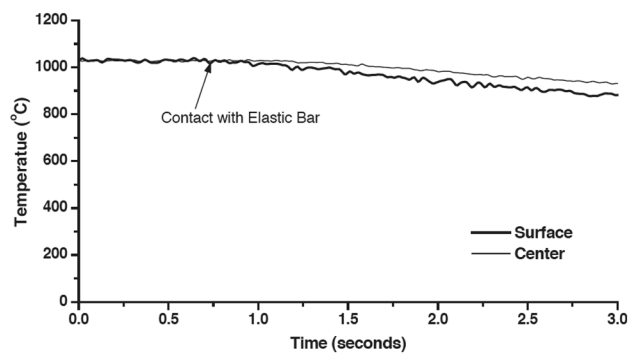
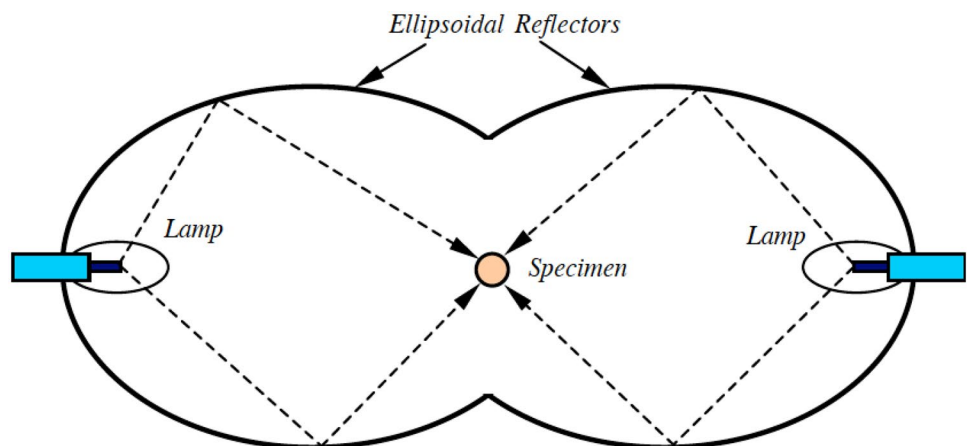


Fig. 9 Temperature–time plot of cooling of a specimen heated to 1025 °C after bringing into contact with cold bars. From [22]

Empirical Check

I have performed an empirical check on whether stress pulses really do propagate from the input to the output bar through both a negative and a positive temperature gradient without significant distortion (see Figs. 13, 14). The bars were 12.7 mm in diameter and 0.5 m long. The strain gauges were positioned half way along the bars. I performed the

Fig. 7 Lamp heating method for heating specimen. From [22]



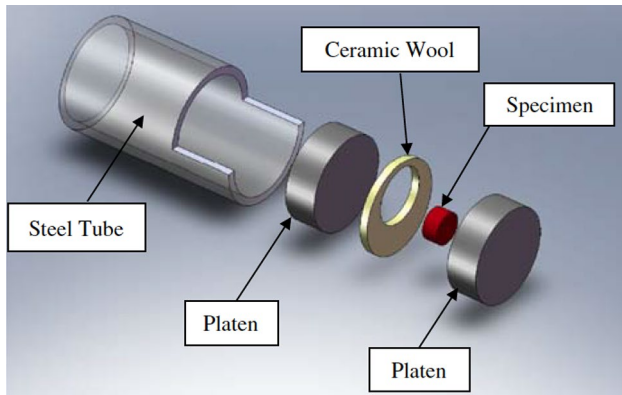


Fig. 10 Metal platen system for shielding the specimen from the cooling effect of the cold bars. From [68]

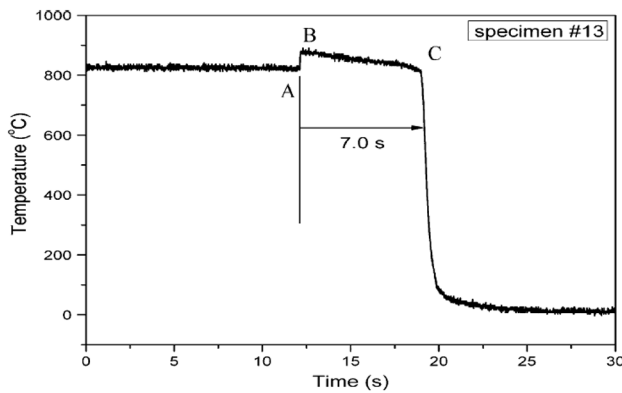


Fig. 11 Temperature–time plot for a steel specimen loaded in the arrangement shown in Fig. 10. The specimen can be seen to remain at the desired test temperature up until loading at which point it rises in temperature due to adiabatic plastic work. From [68]

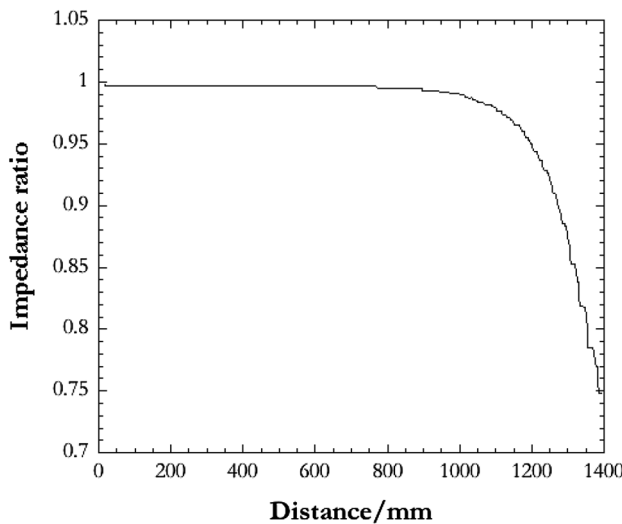
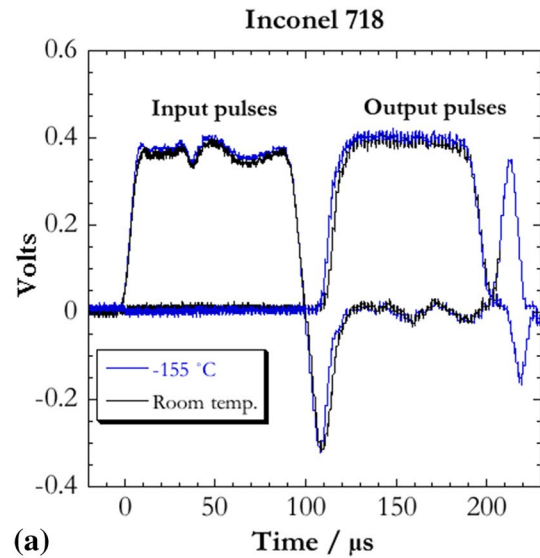
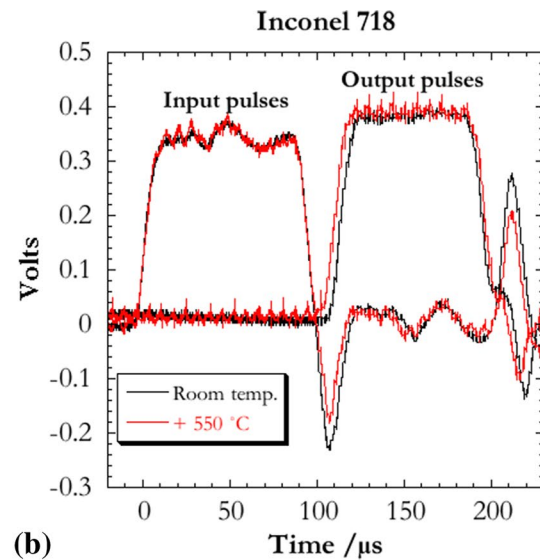


Fig. 12 Impedance as a function of position for an austenitic steel rod heated to 950 °C at the right-hand end. From [24]



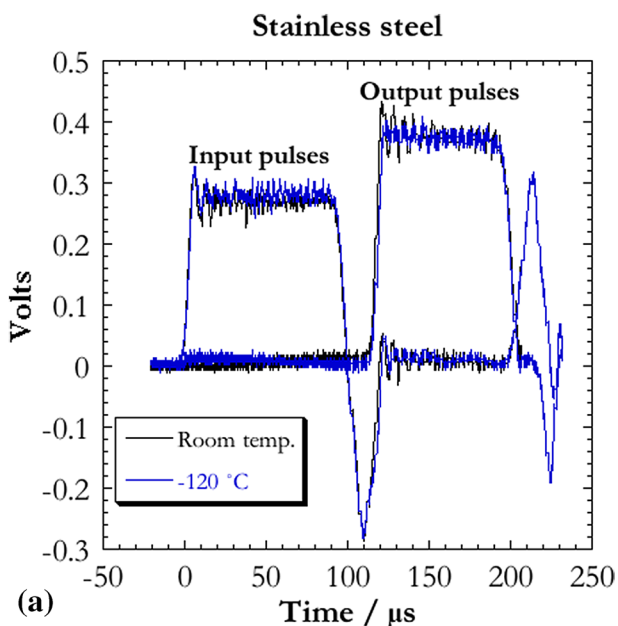
(a)



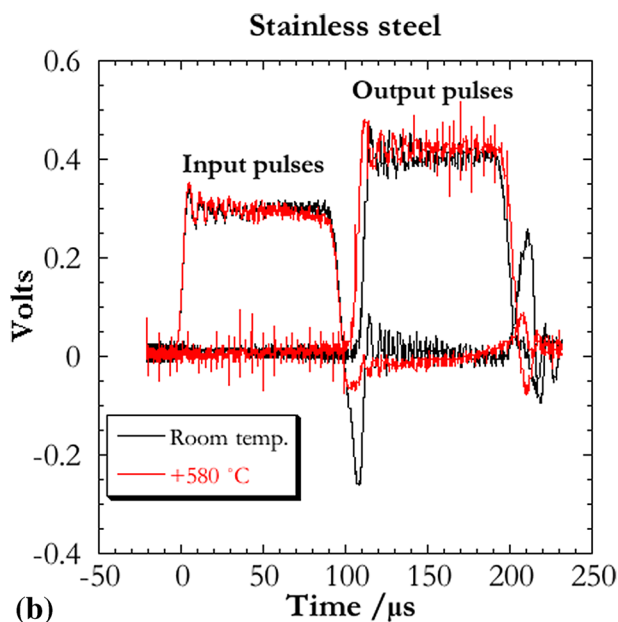
(b)

Fig. 13 Comparison of propagation of pulses from the input bar into the output bar when **a** the interface is at $-155\text{ }^{\circ}\text{C}$ and **b** the interface is at $+550\text{ }^{\circ}\text{C}$ with the same experiment carried out at room temperature when both bars are made from Inconel 718

check by comparing the output bar pulses obtained when the whole apparatus was at room temperature with those obtained where both bar ends were either cold or hot. The only visible effect of the temperature gradient is a slight time shift in the output pulses (a similar observation was made recently by Potter et al. [72]). Note that the ‘spikes’ that can be seen on the traces obtained at high temperatures are due to the induction heater used. No visible distortion of the pulses can be seen except for one experiment where the input pulse shows a ‘rounded knee’ at around 90 μs at high temperature (Fig. 14b). This is probably due to elastic wave energy being reflected from the temperature gradient (cf.



(a)



(b)

Fig. 14 Comparison of propagation of pulses from the input bar into the output bar when **a** the interface is at $-120\text{ }^{\circ}\text{C}$ and **b** the interface is at $+580\text{ }^{\circ}\text{C}$ with the same experiment carried out at room temperature when both bars are made from stainless steel

Fig. 3). It should be noted that another test under the same conditions with stainless steel bars did not show this phenomenon. We may conclude therefore that stainless steel can be used for Hopkinson bar work at cryogenic temperatures but is slightly inferior to Inconel 718 for high temperature work.

One way of calculating the impedance as a function of position and the amount of energy reflected from the temperature

gradient is to determine the functional form of the temperature distribution, $T(x)$, along the bar. As most researchers use resistance furnaces (which can take up to 30 min to heat the specimen [43]), the bar is assumed to be in a steady state thermally [24, 43]. These authors also checked the temperature distribution using thermocouples (see Figs. 15, 16). Then to turn this into an impedance versus position graph, the relationship between Young’s modulus and temperature must also be known for the bar material (the effect of temperature on the density of the bar is ignored as being a relatively small effect [24, 25]). This relationship has usually been taken to be linear [23, 24]:

$$E(T) = E_0[1 - \beta(T - T_0)], \tag{1}$$

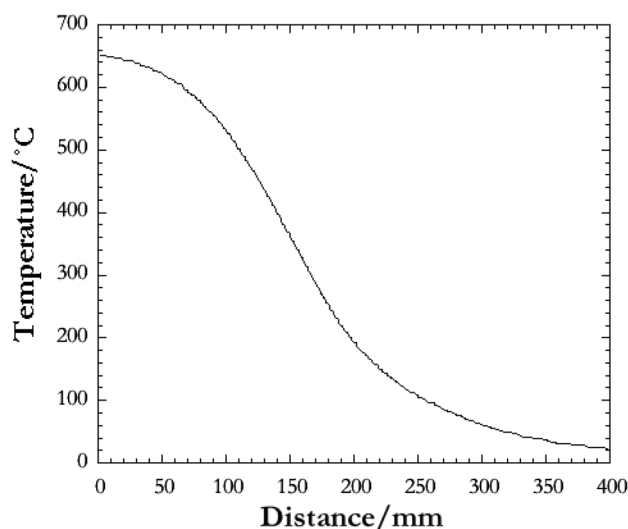


Fig. 15 Temperature distribution in a Hopkinson pressure bar measured using thermocouples placed at 5 cm intervals. From [43]

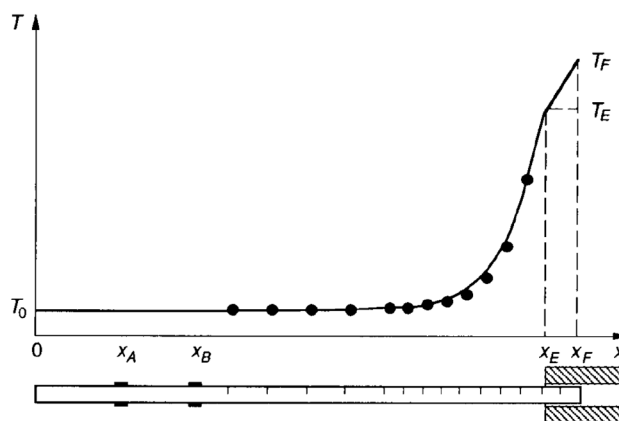


Fig. 16 Temperature distribution in a Hopkinson pressure bar where the end temperature was $950\text{ }^{\circ}\text{C}$. Solid circles are measured values, the solid line was calculated. From [24]

where E_0 is Young's modulus at ambient temperature, β is the measure of the dependence of modulus on temperature (ca. $4 \times 10^{-4} \text{ K}^{-1}$ for steel [25]), and T_0 is the ambient temperature.

Chiddister and Malvern [43] found that approximating the smooth curve shown in Fig. 15 by a set of five discrete temperature steps allowed them to calculate the strain in the specimen to within 1% of the value measured by a strain gauge attached directly to the specimen at temperatures up to 480 °C and to within 3% at 650 °C (the reflection of a stress wave from a set of step changes in modulus can be calculated analytically). This procedure was further checked by comparing the predictions with the measured stress pulse reflected back down the input bar.

Bacon et al. [24] found that solving the one-dimensional heat equation gave almost the same answer as solving the two-dimensional heat equation (assuming that the heat flux down the bar is constant down the bar and that the temperature gradient inside the furnace is linear). Both solutions lay close to the temperature values they measured (see Fig. 16). They quote the 1D solution for $T(x)$ as follows:

$$T_0, \quad x \leq x_B,$$

$$T(x) = (T_E - T_0) \frac{\sinh \mu (x - x_B)}{\sinh \mu (x_E - x_B)} + T_0, \quad x_B \leq x \leq x_E, \quad (2)$$

$$\frac{T_F (x - x_E) + T_E (x_F - x)}{x_F - x_E}, \quad x \geq x_E,$$

where the temperature and position variables are defined in Fig. 16. μ is a parameter that the authors defined as $\mu = 2h/a\lambda$ where h is the heat flux, λ is the thermal conductivity, and a is the radius of the rod. The definition of mechanical impedance $Z = \sqrt{\rho E}$, where ρ is the bar density (taken to be constant), and so

$$Z(x) = Z_0 [1 - \beta (T(x) - T_0)]^{0.5}, \quad (3)$$

where Z_0 is the impedance at room temperature.

A method that can be used to determine $Z(x)$ directly is the two-point measurement technique developed by Lundberg et al. [70, 71, 73] whose original use was for bars having a cross-section that varies with position. The technique involves measuring the strain pulses at two points A and B remote from the furnace (see Fig. 16). Then by dividing up the bar between B and the end into equal segments (40 were used in the calculation performed by Bacon et al. [24]), expressions can be derived for the force and particle velocity at the entrance to each segment [making the assumption that the functional form of $Z(x)$ is as given in Eqs. (2) and (3)] until the end of the bar is reached. If the end of the bar is free,

the force there must be zero. This boundary condition was then applied in a minimization routine to determine $Z(x)$, and this is plotted in Fig. 12.

Bacon et al. [24] also performed an experimental check to see whether their theory correctly predicted the force pulse measured on an extension rod brought into contact with the main rod just before a force pulse was launched down it. The agreement was found to be much better than assuming the impedance did not vary with position, though there was a small residual error in calculating the time at which the particle velocity began to rise (the time at which the force pulse began to rise was correctly predicted). They attributed this discrepancy (equivalent to a displacement of 10 μm) to imperfect contact between the two bars.

Conclusions

The method developed by Bacon et al. [24] can be applied to any temperature distribution expressible in polynomial form. The problem with applying their technique to cases where the specimen is heated (or cooled) very rapidly is that the heat flux in the bar is not in a steady state. This means that the functional form of the temperature distribution may not be calculable from the heat diffusion equation: indeed it may vary from shot to shot. Whether a good enough approximation can be arrived at is a matter for future investigators to determine.

Acknowledgements I thank the referees for their helpful suggestions for improving the paper.

Open Access This article is licensed under a Creative Commons Attribution 4.0 International License, which permits use, sharing, adaptation, distribution and reproduction in any medium or format, as long as you give appropriate credit to the original author(s) and the source, provide a link to the Creative Commons licence, and indicate if changes were made. The images or other third party material in this article are included in the article's Creative Commons licence, unless indicated otherwise in a credit line to the material. If material is not included in the article's Creative Commons licence and your intended use is not permitted by statutory regulation or exceeds the permitted use, you will need to obtain permission directly from the copyright holder. To view a copy of this licence, visit <http://creativecommons.org/licenses/by/4.0/>.

References

1. Sjöberg T, Sundin KG, Kajberg J, Oldenburg M (2016) Reverse ballistic experiment resembling the conditions in turbine blade off event for containment structures. *Thin Walled Struct* 107:671–677
2. Han Y, Soltis J, Palacios J (2018) Engine inlet guide vane ice impact fragmentation. *AIAA J* 56:3680–3690
3. Kristoffersen M, Hauge KO, Valsamos G, Børvik T (2018) Blast loading of concrete pipes using spherical centrally placed C-4 charges. *EPJ Web Conf* 183:01057

4. Roy PP, Sawmliana C, Singh RK, Chakunde VK (2012) Effective blasting using mixture of ammonium nitrate, fuel oil, sawdust and used oil at limestone mine. *Min Technol* 121:46–51
5. Zerilli FJ, Armstrong RW (1987) Dislocation-mechanics-based constitutive relations for materials dynamics calculations. *J Appl Phys* 61:1816–1825
6. Follansbee PS, Kocks UF (1988) A constitutive description of the deformation of copper based on the use of the mechanical threshold stress as an internal state variable. *Acta metall* 36:81–93
7. Church PD, Andrews T, Goldthorpe B (1999) A review of constitutive model development within DERA. In: Jerome DM (ed) *Structures under extreme loading conditions PVP 394*. American Society of Mechanical Engineers, New York, pp 113–120
8. Williamson DM, Siviour CR, Proud WG, Palmer SJP, Govier R, Ellis K, Blackwell P, Leppard C (2008) Temperature–time response of a polymer bonded explosive in compression (EDC37). *J Phys D* 41:085404
9. Siviour CR, Jordan JL (2016) High strain rate mechanics of polymers: a review. *J Dyn Behav Mater* 2:15–32
10. Lea LJ, Jardine AP (2018) Characterisation of high rate plasticity in the uniaxial deformation of high purity copper at elevated temperatures. *Int J Plast* 102:41–52
11. Chen W, Song B (2011) Kolsky compression bar experiments at high/low temperatures. *Split Hopkinson (Kolsky) bar: design, testing and applications*. Springer, New York, pp 233–260
12. Chen W, Song B (2011) *Split Hopkinson (Kolsky) bar: design, testing and applications*. Springer, New York
13. Sawas O, Brar NS, Brockman RA (1998) Dynamic characterization of compliant materials using an all-polymeric split Hopkinson bar. *Exp Mech* 38:204–210
14. Bacon C, Brun A (2000) Methodology for a Hopkinson bar test with a non-uniform viscoelastic bar. *Int J Impact Eng* 24:219–230
15. Yao L (2016) Experimental and numerical study of dynamic crack propagation in ice under impact loading. PhD thesis, University of Lyon, France
16. Williams ML, Landel RF, Ferry JD (1955) The temperature dependence of relaxation mechanisms in amorphous polymers and other glass-forming liquids. *J Am Chem Soc* 77:3701–3707
17. Yunoshev AS, Silvestrov VV (2001) Development of the polymeric split Hopkinson bar technique. *J Appl Mech Tech Phys* 42:558–564
18. Tamaogi T, Sogabe T (2015) Viscoelastic properties for PMMA bar over a wide range of frequencies. In: Qi HJ, Antoun B, Hall R, Lu H, Arzounanidis A, Silberstein M, Furmanski J, Amirkhizi A, Gonzalez-Gutierrez J (eds) *Challenges in mechanics of time-dependent materials*. Springer, New York, pp 95–100
19. Kendall MJ, Siviour CR (2014) Experimentally simulating high-rate behaviour: rate and temperature effects in polycarbonate and PMMA. *Philos Trans R Soc A* 372:20130202
20. Gray GT III, Blumenthal WR (2000) Split-Hopkinson pressure bar testing of soft materials. In: Kuhn H, Medlin D (eds) *ASM handbook*. ASM International, Materials Park, pp 488–496
21. Gray III GT, Idar DJ, Blumenthal WR, Cady CM, Peterson PD (2000) High- and low-strain rate compression properties of several energetic material composites as a function of strain rate and temperature. In: Short JM, Kennedy JE (eds) *Proceedings of the 11th international detonation symposium*. Office of Naval Research, Arlington, pp 76–84
22. Seo S, Min O, Yang H (2005) Constitutive equation for Ti6Al4V at high temperatures measured using the SHPB technique. *Int J Impact Eng* 31:735–754
23. Lindholm US, Yeakley LM (1968) High strain rate testing: tension and compression. *Exp Mech* 8:1–9
24. Bacon C, Carlsson J, Lataillade J-L (1991) Evaluation of force and particle velocity at the heated end of a rod subjected to impact loading. *J Phys IV* 1(C3):395–402
25. Bacon C (1993) Numerical prediction of the propagation of elastic waves in longitudinally impacted rods: applications to Hopkinson testing. *Int J Impact Eng* 13:527–539
26. Loshmanov LP, Nechaeva OA, Rudnev VD (1996) High-speed tests at elevated temperatures. *Ind Lab* 62:311–313
27. Kolsky H (1953) *Stress waves in solids*. Clarendon Press, Oxford
28. Stanford EG (1950) A contribution on the velocity of longitudinal elastic vibrations in cylindrical rods, and on the relationship between Young's modulus and temperature for aluminium. *Nuovo Cimento Suppl (Ser 9)* 7:332–340
29. Datta AN (1956) Longitudinal propagation of elastic disturbance for linear variations of elastic parameters. *Indian J Theor Phys* 4:43–50
30. Sur SP (1961) A note on the longitudinal propagation of elastic disturbance in a thin inhomogeneous elastic rod. *Indian J Theor Phys* 9:61–67
31. Lindholm US, Doshi KD (1965) Wave propagation in an elastic nonhomogeneous bar of finite length. *Trans ASME J Appl Mech* 32:135–142
32. Whittier JS (1965) A note on wave propagation in a nonhomogeneous bar. *Trans ASME J Appl Mech* 32:947–949
33. Francis PH (1966) Wave propagation in thin rods with quiescent temperature gradients. *Trans ASME J Appl Mech* 33:702–704
34. Francis PH (1967) Note on the propagation of elastic waves in a nonhomogeneous rod of finite length. *Trans ASME J Appl Mech* 34:226–227
35. Gorham DA, Pope PH, Cox O (1984) Sources of error in very high strain rate compression tests. *Inst Phys Conf Ser* 70:151–158
36. Dally JW, Riley WF (1987) Strain gages. In: Kobayashi AS (ed) *Handbook on experimental mechanics*. Prentice-Hall, Englewood Cliffs, pp 41–78
37. Strand OT, Goosman DR, Martinez C, Whitworth TL, Kuhlrow WW (2006) Compact system for high-speed velocimetry using heterodyne techniques. *Rev Sci Instrum* 77:083108
38. Avinadav C, Ashuach Y, Kreif R (2011) Interferometry-based Kolsky bar apparatus. *Rev Sci Instrum* 82:073908
39. Lea LJ, Jardine AP (2016) Application of photon Doppler velocimetry to direct impact Hopkinson pressure bars. *Rev Sci Instrum* 87:023101
40. Rosenberg Z, Dawicke D, Bless SJ (1986) A new technique for heating specimens in split Hopkinson bar experiments using induction coil heaters. In: Murr LE, Staudhammer KP, Meyers MA (eds) *Metallurgical applications of shock wave and high strain rate phenomena*. Marcel Dekker, New York, pp 543–552
41. Rosenberg Z, Dawicke D, Strader E, Bless SJ (1986) A new technique for heating specimens in split-Hopkinson-bar experiments using induction coil heaters. *Exp Mech* 26:275–278
42. Macdougall DAS, Harding J (1998) The measurement of specimen surface temperature in high-speed tension and torsion tests. *Int J Impact Eng* 21:473–488
43. Chiddister JL, Malvern LE (1963) Compression-impact testing of aluminum at elevated temperatures. *Exp Mech* 3:81–90
44. Eleiche AM, Duffy J (1975) Effects of temperature on the static and dynamic stress–strain characteristics in torsion of 1100-0 aluminum. *Int J Mech Sci* 17:85–95
45. Frantz CE, Follansbee PS, Wright WT (1984) Experimental techniques with the SHPB. In: Berman I, Schroeder JW (eds) *High energy rate fabrication: 1984*. American Society of Mechanical Engineers, New York, pp 229–236
46. Gálvez F, Cendón D, Sánchez-Gálvez V (2005) Ensayos mecánicos en materiales a elevada velocidad de deformación y alta temperatura. *Ann Mec Fract* 22:508–513

47. Gálvez F, Cendón D, Enfedaque A, Sánchez-Gálvez V (2006) High strain rate and high temperature behaviour of metallic materials for jet engine turbine containment. *J Phys IV Fr* 134:269–274
48. Krafft JM, Sullivan AM, Tipper CF (1954) The effect of static and dynamic loading and temperature on the yield stress of iron and mild steel in compression. *Proc R Soc Lond A* 221:114–127
49. Samanta SK (1971) Dynamic deformation of aluminium and copper at elevated temperatures. *J Mech Phys Solids* 19:117–135
50. Campbell JD, Dowling AR (1970) The behaviour of materials subjected to dynamic incremental shear loading. *J Mech Phys Solids* 18:43–63
51. Campbell JD, Ferguson WG (1970) The temperature and strain rate dependence of the shear strength of mild steel. *Philos Mag* 21:63–82
52. Senseny PE, Duffy J, Hawley RH (1978) Experiments on strain rate history and temperature effects during the plastic deformation of close-packed metals. *Trans ASME J Appl Mech* 45:60–66
53. Kishida K, Kataoka T, Yokoyama T, Nakano M (1987) Behaviour of materials at high strain rates and cryogenic temperature. In: Kawata K, Shioiri J (eds) *Macro- and micro-mechanics of high velocity deformation and fracture*. Springer, Berlin, pp 75–84
54. Kandasamy R, Brar NS (1994) Flow stress and material model study at high strain rate and low temperature. *AIP Conf Proc* 309:1031–1034
55. Lennon AM, Ramesh KT (1998) A technique for measuring the dynamic behavior of materials at high temperatures. *Int J Plast* 14:1279–1292
56. Basak D, Yoon HW, Rhorer R, Burns TJ, Matsumoto T (2004) Temperature control of pulse heated specimens in a Kolsky bar apparatus using microsecond time-resolved pyrometry. *Int J Thermophys* 25:561–574
57. Mates SP, Rhorer R, Whitenon E, Burns T, Basak D (2008) A pulse-heated Kolsky bar technique for measuring the flow stress of metals at high loading and heating rates. *Exp Mech* 48:799–808
58. Hueto F, Hokka M, Sancho R, Rämö J, Östman K, Gálvez F, Kuokkala V-T (2017) High temperature dynamic tension behavior of titanium tested with two different methods. *Procedia Eng* 197:130–139
59. Song B, Chen WN, Yanagita T, Frew DJ (2005) Temperature effects on the dynamic compressive properties of an epoxy syntactic foam. *Compos Struct* 67:289–298
60. Greaves RH, Jones JA (1926) The ratio of the tensile strength of steel to the Brinell hardness number. *J Iron Steel Inst* 113:335–353
61. Tabor D (1948) A simple theory of static and dynamic hardness. *Proc R Soc Lond A* 192:247–274
62. Tabor D (1951) *The hardness of metals*. Clarendon Press, Oxford
63. Apostol M, Vuoristo T, Kuokkala V-T (2003) High temperature high strain rate testing with a compressive SHPB. *J Phys IV Fr* 110:459–464
64. Sizek HW, Gray GT III (1993) Deformation of polycrystalline Ni₃Al at high strain rates and elevated temperatures. *Acta metall mater* 41:1855–1860
65. Gray III GT (2000) Classic split-Hopkinson pressure bar testing. In: Kuhn H, Medlin D (eds) *ASM handbook. Mechanical testing and evaluation*, vol 8. ASM International, Materials Park, pp 462–476
66. Lankford J (1977) Compressive strength and microplasticity in polycrystalline alumina. *J Mater Sci* 12:791–796
67. Lankford J (1981) Temperature–strain rate dependence of compressive strength and damage mechanisms in aluminium oxide. *J Mater Sci* 16:1567–1578
68. Song B, Antoun BR, Nie X, Chen W (2010) High-rate characterization of 304L stainless steel at elevated temperatures for recrystallization investigation. *Exp Mech* 50:553–560
69. Bacon C (1993) *Mesure de la tenacité dynamique de matériaux fragiles en flexion-trois-points à haute température: Utilisation des barres de Hopkinson*. PhD Thesis, University of Bordeaux I
70. Lundberg B, Henchoz A (1977) Analysis of elastic waves from two-point strain measurement. *Exp Mech* 17:213–218
71. Lundberg B, Carlsson J, Sundin KG (1990) Analysis of elastic waves in non-uniform rods from two-point strain measurement. *J Sound Vib* 137:483–493
72. Potter RS, Cammack JM, Braithwaite CH, Walley SM (2019) Problems associated with making mechanical measurements on water-ice at quasistatic and dynamic strain rates. *J Dyn Behav Mater* 5:198–211
73. Lundberg B, Blanc RH (1988) Determination of mechanical material properties from the two-point response of an impacted linearly viscoelastic rod specimen. *J Sound Vib* 126:97–108

Publisher's Note Springer Nature remains neutral with regard to jurisdictional claims in published maps and institutional affiliations.